Structure and Dynamics of 9(10H)-Acridone and Its Hydrated Clusters. II. Structural Characterization of Hydrogen-Bonding Networks

Masaaki Mitsui[†] and Yasuhiro Ohshima*

Department of Chemistry, Graduate School of Science, Kyoto University, Kitashirakawa-Oiwakecho, Sakyo-ku, Kyoto 606-8502, Japan

Shun-ichi Ishiuchi,[‡,§] Makoto Sakai,[‡] and Masaaki Fujii[‡,§]

Institute for Molecular Science, Myodaiji, Okazaki 444-8585, Japan and Department of Functional Molecular Science, School of Mathematical and Physical Science, Graduate University for Advanced Studies, Myodaiji, Okazaki 444-8585, Japan

Received: March 20, 2000; In Final Form: July 5, 2000

The present paper represents fluorescence-detected infrared measurements of 9(10H)-acridone (AD) and 10 of its fluorescent hydrated clusters, AD−$(H_2O)_n$ (n = 1−5 and more), which have been performed by monitoring the fluorescence from their $^1(\pi,\pi^*)$ electronic origin transitions reported in paper I. In the $n = 1$ and 2 clusters, free N−H stretching band has been identified in addition to O−H stretching bands characteristic to water molecules acting as single proton donors. As the next solvation step, the H-bonded O−H stretches are further developed in the red-shifted region and the N−H stretch becomes involved in the hydrogen-bonds for the $n = 3-5$ clusters. For $n \geq 6$, more than one pair of double-donor O−H stretches appear. These spectral features are well correlated to the stepwise evolution in the hydrogen-bonding networks in AD−$(H_2O)_n$, which have been predicted by the (π,π^*) spectral-shift analysis and DFT calculations presented in paper I: water units are bound to the C═O site for $n = 1$ and 2, a single water chain bridges between the C═O and N−H sites above the AD aromatic rings for $n = 3-5$, and water bridges become branched for $n \geq 6$ and probably form three-dimensional cages at higher aggregation levels. Differences in hydrogen-bonding topologies, stabilities, and dynamical behaviors among the conformers are discussed on the basis of the experimental observations, the DFT calculations, and comparison with other hydrated aromatic clusters.

1. Introduction

As a part of an investigation aiming at clarifying a relation between solvation structure and intracluster dynamics, the preceding paper (paper I) has presented electronic spectroscopy and DFT calculations of 9(10H)-acridone (AD) and its hydrated clusters, AD−$(H_2O)_n$. From the fluorescence-excitation measurements, only a single isomeric form has been identified for each cluster size ranging from $n = 1$ to 5. On the other hand, DFT structural optimizations at the B3LYP/6-31G(d,p) level have yielded several minimum-energy conformations for every cluster size. As AD has multiple hydrogen-bonding sites, the identified isomers show a variety of solvation topologies. The C═O and N−H bonded forms are found for $n = 1$ and 2, and water units become able to make a bridge between the two sites as another water is added. For $n \geq 3$, there exist two further possibilities (chain-type or cyclic-type) for water units bound to AD. For a given cluster size, calculated binding energies of several different conformers are quite close to each other. Hence it is practically impossible to carry out the assignments of the observed species by considering only the calculated stabilities at the present level. Therefore, we have estimated complexation-induced spectral shifts in the $^1(\pi,\pi^*)$ transition as HOMO−LUMO energy differences and compared them with the experimentally determined shifts. For $n = 3-5$, only the bridged form shows a good match-up, but we still need more experimental information to distinguish the two possibilities (i.e., C═O or N−H bonded forms) for $n = 1$ and 2 because of the similarity in their calculated shifts. We must also gain some insights on H-bonding topologies for larger clusters, for which extensive calculations are highly demanding.

As has been mentioned briefly in paper I, vibrational spectroscopy implemented with a double-resonance (DR) detection scheme is a powerful tool for figuring out supramolecular structures of molecular clusters.[1] In particular, H-bonding topologies in hydrated clusters are sensitively probed via infrared (IR) spectra associated with hydride stretching fundamentals, as O−H stretches of waters exhibit frequency shifts characteristic to the H bonding in which the solvents are involved.[2,3] IR spectra for smaller size clusters are almost self-explanatory. When the spectral patterns are too complicated to be analyzed by themselves, as is often the case for larger clusters, ab initio and/or density functional theory (DFT) computations are to be invoked. The calculations provide crucially important outputs on possible geometries, e.g., structural parameters, binding energies, and frequencies and intensities of all the vibrational modes. By comparing the theoretical results, we can tell with much confidence which geometries are actually observed. Therefore, complementary utilization of IR DR spectroscopy

* Corresponding author. Fax: +81-75-753-3974. E-mail: ohshima@kuchem.kyoto-u.ac.jp.

† Research Fellow of the Japan Society for the Promotion of Science for Young Scientist, 1997−1999.

‡ Institute for Molecular Science.

§ Graduate University for Advanced Studies.

10.1021/jp0010482 CCC: $19.00
Published on Web 08/31/2000

and ab initio and/or DFT calculations has been recently performed by many groups,[4−18] and an understanding of cluster geometry is now steadily and rapidly progressing in various systems. At the present stage, aromatic clusters solvated with up to eight waters have been studied, and novel 3D topologies, i.e., caged and cubic forms, of the H-bonding water networks are identified.[5,8,15] Hydrated clusters of multifunctional molecules also come to be actively studied.[10,12,13,16,17] The IR-DR method has an another advantage of species-selectivity based on its DR nature, which detects the IR transition as enhancement or depletion in electronic excitation monitored by fluorescence or resonance-enhanced ionization. This allows us to distinguish the conformations of different species on a vibronic band-to-band basis, which is indispensable for explicit connection of the excited-state dynamics to the cluster geometry.

This paper represents the results of structural characterizations of the fluorescent hydrated AD clusters by applying fluorescence-detected infrared spectroscopy (FDIRS). Analyses of the observed FDIR spectra and conclusive structural assignments have been performed for relatively smaller-size clusters (n = 1−5), with the aid of various computational outputs from DFT calculations at the B3LYP/6-31G(d,p) level. Some characteristics in H-bonding topologies of larger-size clusters are also revealed via observed FDIR spectra. On the basis of the experimental and theoretical attainments, detailed discussions are presented on marked differences between the water-solvation structures associated to the contrasting two possible bonding sites in AD, i.e., H-donating N−H and H-accepting C═O. These present results are compared with previous studies on other aromatic hydrates. The evolution of H-bonding networks in hydrated AD clusters given here will be used as a firm basis for discussions on changes in electronic-energy levels and remarkable size dependence in nonradiative dynamics of the AD chromophore, explored by various frequency- and time-domain experiments described in the following paper (paper III).

2. Experimental and Computational Procedures

Details of the experimental setup for FDIRS have been presented elsewhere.[18,19] Briefly, tunable IR light in the 2800−3800 cm^{-1} region was generated via difference frequency mixing (DFM) of the second harmonic of a Nd^+:YAG laser (Continuum, Powerlite 8010) and the output of a dye laser (Lumonics, HD-500) pumped by the same Nd^+:YAG laser. An autotracking unit (Inrad, AT-III) with a $LiNbO_3$ crystal was used for DFM. The electronic excitation of the clusters was performed with a frequency doubled output of another Nd^+:YAG laser-pumped dye laser (Spectra Physics, GCR-170/Lumonics, HD-500). The IR and UV laser beams were introduced into a chamber in a counterpropagated direction with each other. The IR laser irradiated the sample prior to the UV laser pulse by ≈50 ns. FDIRS in this study was conducted in a conventional fluorescence depletion scheme: decrease in the ground-state population induced by the IR excitation was monitored through fluorescence by the UV light fixed at the origin band of the clusters. The alternative data acquisition[20] was employed to reduce the long-term fluctuation in the FDIR spectrum.

Ab initio and density-functional-theory (DFT) molecular-orbital calculations of AD and its hydrated clusters have been carried out with a suite of Gaussian 98 programs.[21] Details of the computational procedure have been described in paper I.

3. Experimental Results

FDIR spectra in the 2900−3800 cm^{-1} region have been obtained for bare AD and 10 of its hydrates (i.e., species other than G, I, and K) identified in the fluorescence-excitation spectrum (see paper I) by monitoring their $^1(\pi,\pi^*)$ electronic origin transitions. They are presented in Figure 1. Species A shows a single sharp band at 3478 cm^{-1}, which is definitely assigned to the N−H stretching fundamental. As no other bands have been identified, the species contains no water molecule, confirming its assignment as bare AD. In the FDIR spectra of the hydrated clusters, most of the observed vibrational bands correspond to the N−H stretch of AD or O−H stretches of the solvents. Their vibrational frequencies are summarized in Table 1 for species A−F (n = 0−5). Weak features due to the C−H stretches in the AD chromophore are also observed at ≈3080 cm^{-1} for some species (not included in the table). An overview of the IR spectra for the hydrated AD clusters shows characteristic changes in spectral features as cluster sizes become larger, which indicates stepwise evolution in the H-bonding networks as increasing degrees of solvation. The spectra can be classified into three types for different sizes, i.e., (i) species B and C (n = 1 and 2), (ii) species D−F (n = 3−5), and (iii) species H−N ($n \geq 6$).

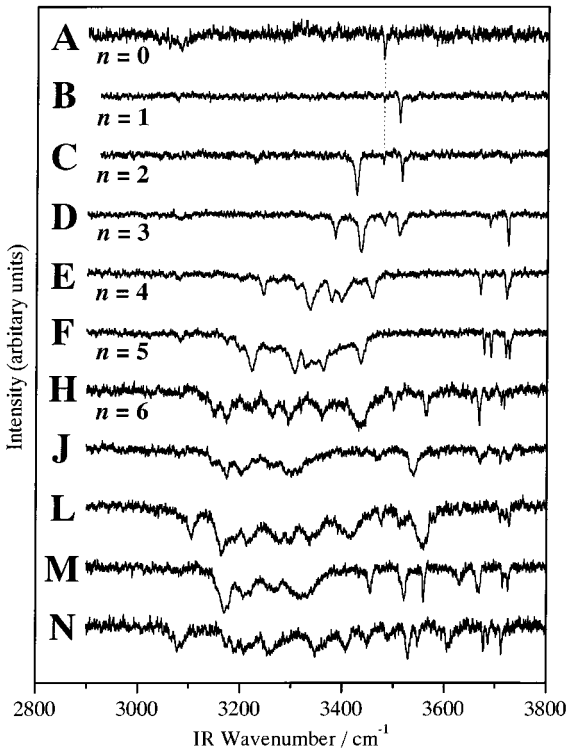

Figure 1. Overview of FDIR spectra for bare AD and its hydrated clusters, AD−$(H_2O)_n$. A−F, J, L, M, and N correspond to the species identified in the fluorescence-excitation spectrum shown in paper I (Figure 1). Species A is bare AD, B−F are the n = 1−5 clusters, respectively, and H is the n = 6 cluster. J, L, M, and N are higher-size clusters with n > 6. All of the FDIR spectra were obtained by monitoring the fluorescence of their $^1(\pi,\pi^*)$ origin bands. N−H stretch vibrations in species B and C are located at the same frequency as bare AD, as connected with dotted lines, whereas no correspondence appears in other species. For most of higher-size clusters as well as the monomer, hole-burning IR laser power had to be increased so as to give an acceptable signal-to-noise ratio, and thus their spectra suffer from saturation effects.

The first type is of the clusters with relatively smaller sizes, n = 1 and 2 (Figure 1, B and C). For these species, a weak band is observed at almost the same frequency as the N−H stretching fundamental of bare AD. As is more thoroughly discussed in the next section, these bands have been confirmed as the N−H stretching fundamental, indicating that H bonding between water and the N−H group of AD is *not* formed in these

TABLE 1: Observed and Calculated Vibrational Frequencies (cm^{-1}) and Calculated IR Intensities (km/mol) of N−H and O−H Stretching Vibrations in Acridone−$(H_2O)_n$ with $n = 0-5$

	vibrational freq.		freq. shift[b]		
species	obs	calc[a]	obs	calc[a]	assignment[c]
bare AD	3478	3637 (38)	−229	−220	N−H
$n = 1$	3479	3635 (49)	−228	−222	Free NH
	3510	3664 (447)	−197	−193	SD
	3729	3865 (68)	+23	+8	F
$n = 2$	3426	3543 (753)	−281	−314	SD(1)
	3478	3634 (36)	−229	−223	Free NH
	3515	3601 (441)	−192	−256	SD(2)
	3727	3864 (35)	+20	+7	F(1)
	3736	3866 (68)	+29	+9	F(2)
$n = 3$	3385	3370 (310)	−322	−487	NH+/SD(1)+
	3435	3461 (748)	−272	−396	NH+/SD(1)−/SD(2)−
	3481	3548 (217)	−226	−309	SD(1)+/SD(2)−/SD(3)−
	3509	3673 (226)	−198	−184	SD(2)+/SD(3)−
	3688	3872 (39)	−19	+15	π(2)
	3724	3873 (59)	+17	+16	F(3)
		3877 (38)		+20	F(1)
$n = 4$	3243	3247 (432)	−464	−610	NH+/SD(1)+/SD(2)+
	3335	3336 (1418)	−372	−521	NH+/SD(1)−/SD(2)−
	3377	3412 (539)	−330	−445	NH+/SD(1)−/SD(2)+/SD(3)+
	3395	3492 (239)	−312	−365	SD(2)+/SD(3)−/SD(4)−
	3457	3561 (541)	−250	−296	SD(3)+/SD(4)−
	3670	3858 (45)	−37	+1	π(3)
	3722	3871 (58)	+15	+14	F(4)
		3877 (41)		+20	F(1)
		3880 (37)		+23	F(2)
$n = 5$	3222	3128 (584)	−485	−729	NH+/SD(1)+/SD(2)+
	3306	3225 (1940)	−401	−632	NH+/SD(1)−/SD(2)−/SD(3)−
	3327	3306 (842)	−380	−551	NH+/SD(1)−/SD(2)+/SD(3)+
	3345	3385 (254)	−362	−472	SD(2)+/SD(3)−/SD(4)−/SD(5)−
	3362	3463 (277)	−345	−394	SD(3)+/SD(4)−/SD(5)−
	3436	3563 (605)	−271	−294	SD(4)+/SD(5)−
	3678	3849 (61)	−29	−8	π(3)
	3691	3867 (57)	−16	+10	π(4)
	3720	3869 (38)	+13	+12	F(5)
	3727	3873 (38)	+20	+16	F(2)
		3875 (41)		+18	F(1)

[a] Obtained by B3LYP/6-31G(d,p) calculations. IR intensities are given in parentheses. [b] Frequency shift relative to the average of the symmetric and antisymmetric O−H stretching fundamentals of the water monomer (3706.5 cm^{-1} for the experimental value[22] and 3856.6 cm^{-1} as the calculated). [c] SD and F refer to single-donor and free O−H bond stretches, respectively. Stretches associated with O−H bonds bound to the π-clouds of AD aromatic rings are indicated by π. Numbering of water molecules, indicated in Figures 4−7 of paper I, are given in parentheses. ± represent relative phases of vibrational displacements for each O−H bond.

species. Other bands due to the O−H stretch fundamentals of water(s) are divided into two groups: one for the H-bonded O−H bond(s) and the other for the free O−H bond(s). The H-bonded bands are located below 3520 cm^{-1}, while the free O−H bands are weakly observed at around 3700 cm^{-1}. The numbers of the H-bonded bands are the same as the solvent numbers. This observation confirms the size assignment on species C ($n = 2$), to which the mass-resolved measurement cannot afford definitive conclusion, as discussed in paper I. The large red shifts of the H-bonded bands relative to bare water (3657 and 3756 cm^{-1} for ν_1 and ν_3, respectively)[22] indicate that all of the water molecules are involved in strong H bonding (i.e., *not* π-type bonding).[14,18,23] Thus the H-bonding networks of waters in these species should be bound to the carbonyl group of AD.

The larger clusters (species D−F) with $n = 3-5$ show the second-type IR spectra. In particular, the spectra of species E and F are quite similar to each other. More detailed inspection indicates that none of them show a band at the same position as the N−H stretch of bare AD. This apparently indicates that the N−H group becomes involved in H-bonding at this level of hydration. These observations are well correlated with the spectral shift analyses presented in paper I, which have proposed that geometry of all the species is of the same type (i.e., "bridged" form), in which a linear water chain bridges the N−H and C═O sites of AD. We note that the band at 3481 cm^{-1} in the FDIR spectrum of species D ($n = 3$) is located quite close to the N−H stretch of bare AD (3478 cm^{-1}), but this band is somewhat broader (fwhm ≈ 6 cm^{-1}) and slightly blue-shifted from the bare N−H stretch. This band thereby should *not* to be due to the N−H stretch of the AD molecule but to an H-bonded O−H stretch of H_2O. The conclusive assignment of this band will be presented in the next section. The observed IR bands of the $n = 3-5$ clusters are grouped into three types: H-bonded O−H (or N−H) bands, the free O−H bands, and O−H band-(s), which is slightly (≈30−50 cm^{-1}) red-shifted from the free O−H bands (see Figure 1, D−F). The H-bonded O−H stretches are more red-shifted than those in the clusters with $n = 1$ and 2, indicating further development in the H-bonding networks of waters. Besides, slightly red-shifted bands imply that weak H-bonding interactions such as π-H bonds will exist in these species, since vibrational bands associated with such H bonds have often been observed at 3600−3700 cm^{-1}.[3,7,15,24] At this level of aggregation, information from only the FDIR spectra cannot make it clear whether the carbonyl group of AD is also H-bonded as the type (i) or not, and detailed comparison with computational results is necessary to address this.

The FDIR spectra of much larger clusters, i.e., H−N ($n \geq 6$), show a drastic change: strong bands appear in the 3500−3600 cm^{-1} region, where vibrational bands are completely absent in the case of types (i) and (ii). This fact reflects the existence of "double-donor (DD)" water molecule(s) in these

TABLE 2: DFT/B3LYP/6-31G(d,p)-Calculated Vibrational Frequencies (cm^{-1}) of Acridone$-(H_2O)_n$ with $n = 1$ and 2

$n = 1$				$n = 2$							
I C═O bonded		**II** N−H bonded		**I** C═O bonded		**II** N−H bonded		**III** *t*-separately bonded		**IV** *c*-separately bonded	
freq	assign[a]	freq	assign[a]	freq	assign[a]	freq	assign[a]	freq	assign[a]	freq	assign[a]
3635	N−H	3484	N−H	3543	SD(1)	3365	N−H	3475	N−H	3475	N−H
3664	SD	3807	ν_1	3601	SD(2)	3543	SD(1)	3649	SD(1)	3649	SD(1)
3864	F	3921	ν_3	3634	N−H	3741	π(2)	3807	ν_1(2)	3807	ν_1(2)
				3864	F(1)	3875	F(1)	3862	F(1)	3862	F(1)
				3866	F(2)	3881	F(2)	3921	ν_3(2)	3921	ν_3(2)

[a] Assignments of vibrations. SD and F represent single-donor and free O−H bond stretches, respectively. Stretches associated with the O−H bond bound to the π-cloud of AD aromatic rings are indicated by π. ν_1 and ν_3 represent vibrational modes similar to the symmetric and antisymmetric O−H stretches in bare water, respectively. Numbering of water molecules, indicated in Figure 4 of paper I, are given in parentheses.

TABLE 3: DFT/B3LYP/6-31G(d,p)-Calculated Vibrational Frequencies (cm^{-1}) of Acridone$-(H_2O)_n$ with $n = 3$

$n = 3$									
I bridged		**II** C═O bonded chain		**III** N−H bonded chain		**IV** C═O bonded cyclic		**V** N−H bonded cyclic	
freq	assign[a]	freq	assign[a]	freq	assign[a]	freq	assign[a]	freq	assign[a]
3370	*N−H*	3435	SD(2)	3252	*N−H*	3364	*SD(2)*	3377	*SD(1)*
3461	*SD(1)*	3517	SD(1)	3386	*SD(1)*	3478	*SD(3)*	3462	*N−H*
3548	*SD(2)*	3555	SD(3)	3490	*SD(2)*	3627	DDν_1(1)	3485	*SD(3)*
3673	*SD(3)*	3633	N−H	3744	π(3)	3634	N−H	3667	*SD(2)*
3872	F(2)	3868	F(3)	3869	F(3)	3709	DDν_3(1)	3829	π(2)
3873	F(3)	3872	F(1)	3873	F(1)	3862	F(2)	3874	F(3)
3877	F(1)	3877	F(2)	3875	F(2)	3864	F(3)	3878	F(1)

[a] Assignments of vibrations. DDν_1 and DDν_3 represent vibrational modes of double-donor waters, which are similar to the symmetric and antisymmetric O−H stretches in bare water, respectively. Vibrational modes in italic are those of concerted motions of several hydride stretches and only the most dominant stretches contributing to the modes are listed for representative purpose. Other notations are the same in Table 2. Numbering of water molecules, indicated in Figure 5 of paper I, are given in parentheses.

TABLE 4: DFT/B3LYP/6-31G(d,p)-Calculated Vibrational Frequencies (cm^{-1}) of Acridone$-(H_2O)_n$ with $n = 4$ and 5

$n = 4$						$n = 5$					
I bridged		**II** N−H bonded chain		**III** N−H bonded cyclic		**I** bridged		**II** bridged		**III** N−H bonded cyclic	
freq	assign[a]	freq	assign[a]	freq	assign[a]	freq	assign[a]	freq	assign[a]	freq	assign[a]
3247	*N−H*	3230	*N−H*	3155	*SD(1)*	3128	*N−H*	3180	*N−H*	2997	*SD(5)*
3336	*SD(1)*	3341	*SD(2)*	3298	*SD(4)*	3225	*SD(2)*	3263	*SD(2)*	3159	*SD(1)*
3412	*SD(2)*	3435	*SD(1)*	3373	*SD(3)*	3306	*SD(1)*	3356	*SD(1)*	3298	*SD(4)*
3492	*SD(3)*	3491	*SD(3)*	3449	*N−H*	3385	*SD(3)*	3390	*SD(3)*	3400	*SD(3)*
3561	*SD(4)*	3762	π(4)	3550	*SD(2)*	3463	*SD(4)*	3456	*SD(4)*	3424	*N−H*
3858	π(3)	3871	F(4)	3843	π(2)	3563	*SD(5)*	3571	*SD(5)*	3561	*SD(2)*
3871	F(4)	3874	F(1)	3868	F(3)	3849	π(3)	3858	F(5)	3826	π(2)
3877	F(1)	3875	F(3)	3868	F(1)	3867	π(4)	3860	π(4)	3829	π(4)
3880	F(2)	3882	F(2)	3869	F(4)	3869	F(5)	3867	F(1)	3870	F(1)
						3873	F(2)	3873	F(3)	3872	F(5)
						3875	F(1)	3876	F(2)	3875	F(3)

[a] Assignments of vibrations. Other notations are the same in Tables 2 and 3. Numbering of water molecules, indicated in Figures 6 and 7 of paper I, are given in parentheses.

clusters, as the DD O−H stretching vibrations have been located experimentally in this region.[3,5,15] Therefore, the H-bonding networks of waters at this level of aggregation begin to form multiple chains which are connected at the DD water(s). In particular, a number of DD O−H stretches (at least three) are evidently observed in species L−N, which implies development of the H-bonding networks into three-dimensional (3D) forms.

4. Assignments of FDIR Spectra

For more detailed assignments of the observed stretching vibrations and definitive characterizations of cluster geometry, the observed FDIR spectra for the hydrated AD clusters are compared with vibrational frequencies and infrared intensities for minimum-energy structures, which have been calculated at the B3LYP/6-31G(d,p) level of theory as described in paper I. All of the calculated frequencies of the O−H and N−H stretching vibrations for the stable isomers are listed in Table 2 for $n = 1$ and 2, in Table 3 for $n = 3$, and in Table 4 for $n = 4$ and 5. Before the comparisons, as a reference for the solute chromophore in the clusters, geometrical optimization on bare AD has been conducted without any symmetry constraint, which has resulted in a C_{2v} planar structure. The calculated results on its N−H stretch are listed in Table 1. The calculated harmonic frequency exceeds the observed (anharmonic) vibrational frequency by $\approx$160 cm^{-1}, or 4.6%.

Harmonic frequencies of bare H_2O at this level of theory are 3800 and 3913 cm^{-1} for the ν_1 and ν_3 fundamentals, respectively, while the observed frequencies have been reported as 3657 and 3756 cm^{-1}.[22] Because we primarily focus on the *changes* in vibrational properties by cluster formation, comparison of the vibrational frequencies is carried out thoroughly in terms of relative shifts from the average of the monomer ν_1 and ν_3 fundamentals (3706.5 and 3856.6 cm^{-1} for the experiment and calculation, respectively), adopted by Zweir and coworkers.[4]

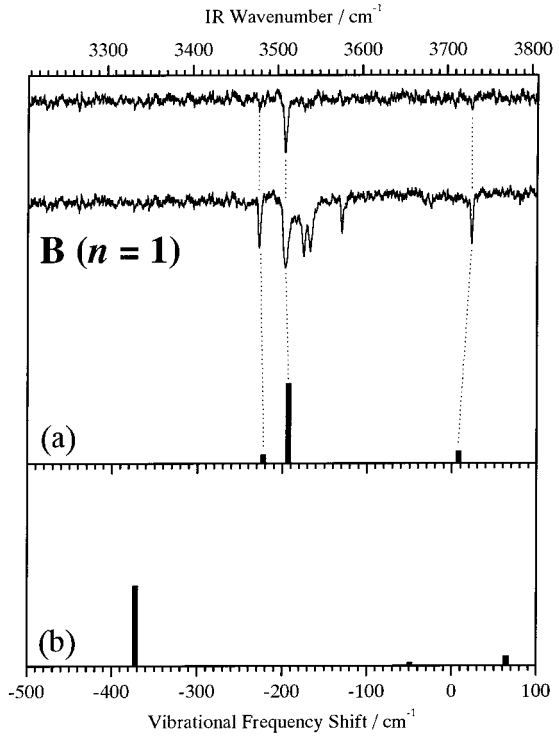

Figure 2. Comparison of the experimental and calculated N−H/O−H vibrational bands for species B [AD−$(H_2O)_1$]. Top two panels show observed FDIR spectra recorded under low and high IR laser powers for the upper and lower traces, respectively. Calculated spectra for the two isomers of $n = 1$ obtained at the B3LYP/6-31G(d,p) level are indicated as stick diagrams: (a) the C═O bonded-type (**I**) and (b) the N−H bonded-type (**II**) (see Figure 3 of paper I). Corresponding vibrational fundamentals in the observed and calculated spectra are connected with dotted lines. The zero of the calculated frequency shift is set at the average of the symmetric and antisymmetric stretching frequencies of bare water at the same level of theory (3856.6 cm^{-1}). Intensities in the calculated IR spectra are normalized as the strongest transitions become the same for the different isomers.

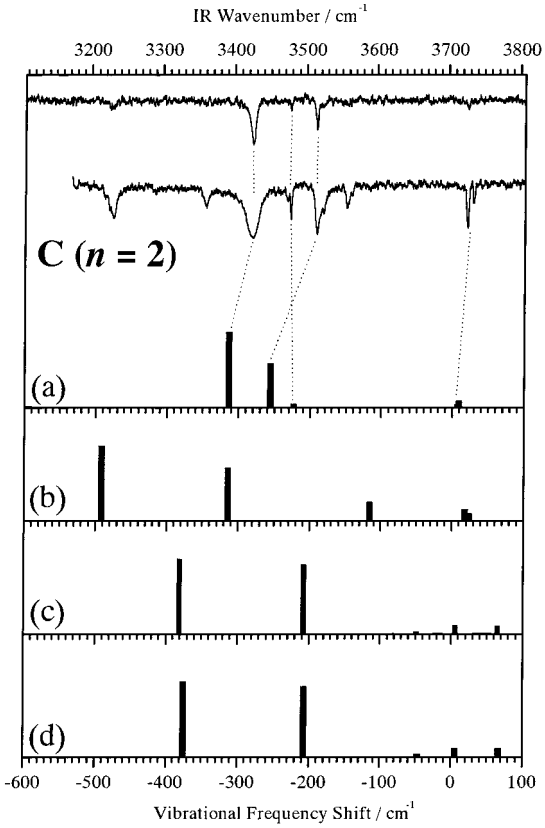

Figure 3. Comparison of the experimental and calculated N−H/O−H vibrational bands for species C [AD−$(H_2O)_2$]. Top two panels show observed FDIR spectra recorded under low and high IR laser powers for the upper and lower traces, respectively. Calculated spectra for the four isomers of $n = 2$ obtained at the B3LYP/6-31G(d,p) level are indicated as stick diagrams: (a) the C═O bonded-type (**I**), (b) the N−H bonded-type (**II**), (c) the *trans*-separately bonded-type (**III**), and (d) the *cis*-separately bonded-type (**IV**) (see Figure 4 of paper I). Other details are the same as in Figure 2.

(1) AD−$(H_2O)_1$. The calculated IR spectra of AD−$(H_2O)_1$ **I** and **II** are indicated as stick diagrams in Figure 2, along with the FDIR spectra of species B recorded under high and low IR laser power conditions. The calculated spectrum of the C═O bonded AD−$(H_2O)_1$ **I** is in extremely good agreement with the spectrum observed with weaker IR laser, which is virtually free from saturation effects. From such an excellent quantitative correspondence, species B is undoubtedly assigned as the C═O bonded-type isomer **I**. This conclusion is consistent with the agreement between the observed spectral shift and the calculated value from the HOMO−LUMO energy gap as mentioned in paper I. The definitive assignments of the O−H and N−H stretches are listed in Table 1. In the observed spectrum with stronger IR power, bands other than the N−H or O−H stretching fundamentals appear at 3532, 3539, and 3576 cm^{-1}. They are probably some combination and/or overtone bands of the AD chromophore.

The calculated N−H stretching band of the N−H bonded AD−$(H_2O)_1$ **II** shows an extremely large red shift of 153 cm^{-1} from bare AD, and its O−H stretching bands are quite similar to those of bare H_2O. It is predicted that this isomer (**II**) is more stable than isomer **I** (see Table 2 in paper I), but it has not been identified in the FE spectrum.

(2) AD−$(H_2O)_2$. The calculated IR spectra for the four stable structures are shown in Figure 3. The calculated spectrum of the C═O bonded AD−$(H_2O)_2$ **I** well reproduces the observed spectrum of species C, though the red shifts in the H-bonded O−H stretches are slightly overestimated. Comparison of the observed and calculated spectra provides definitive assignments of the O−H stretching vibrations, as listed in Table 1. The most red-shifted band at 3426 cm^{-1} with much larger intensity corresponds to the H-bonded O−H stretch of water #1, which is directly attached to AD. The second intense band at 3515 cm^{-1} is of the H-bonded stretch of water #2. As in the case of the species B, i.e., AD−$(H_2O)_1$ **I**, the IR spectrum observed with stronger IR power shows extra bands at 3229, 3360, and 3557 cm^{-1}. In addition, there is a small band just below the peak of the N−H stretch. This observation indicates the existence of anharmonic coupling between the N−H stretching fundamental and other vibrational state(s) with multiple quanta excitations.

In the case of the N−H bonded-type isomer **II**, one of the O−H stretching bands of water #2 appears with the shift of −116 cm^{-1}, which is in the typical range for π-H-bonded O−H stretch fundamentals. Its N−H stretching band is further red-shifted by 272 cm^{-1} from bare AD. IR spectra of the separately bonded isomers **III** and **IV** are almost identical and essentially additions of those of the N−H and C═O bonded AD−$(H_2O)_1$ clusters.

(3) AD−$(H_2O)_3$. Calculated IR spectra for the AD−$(H_2O)_3$ **I**−**V** clusters are shown in Figure 4, along with the observed FDIR spectrum of species D. The assignments of their O−H and N−H stretches are collected in Table 3. From simple comparison, we can exclude the C═O bonded chain-type (**II**) and N−H bonded chain-type (**III**) isomers from the candidates

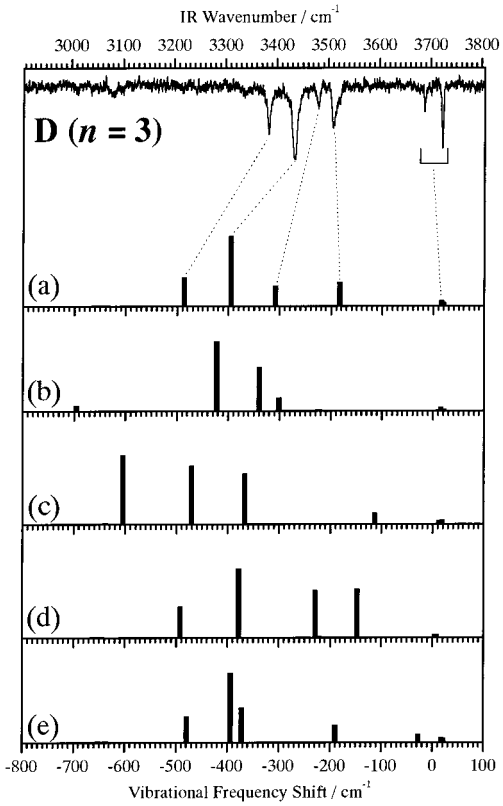

Figure 4. Comparison of the experimental and calculated N−H/O−H vibrational bands for species D [AD−$(H_2O)_3$]. The top panel shows the observed FDIR spectrum, and calculated spectra for the five isomers of $n = 3$ obtained at the B3LYP/6-31G(d,p) level are indicated as stick diagrams: (a) the bridged-type (**I**), (b) the C═O bonded chain-type (**II**), (c) the N−H bonded chain-type (**III**), (d) the C═O bonded cyclic-type (**IV**), and (e) the N−H bonded cyclic-type (**V**) (see Figure 5 of paper I). Other details are the same as in Figure 2.

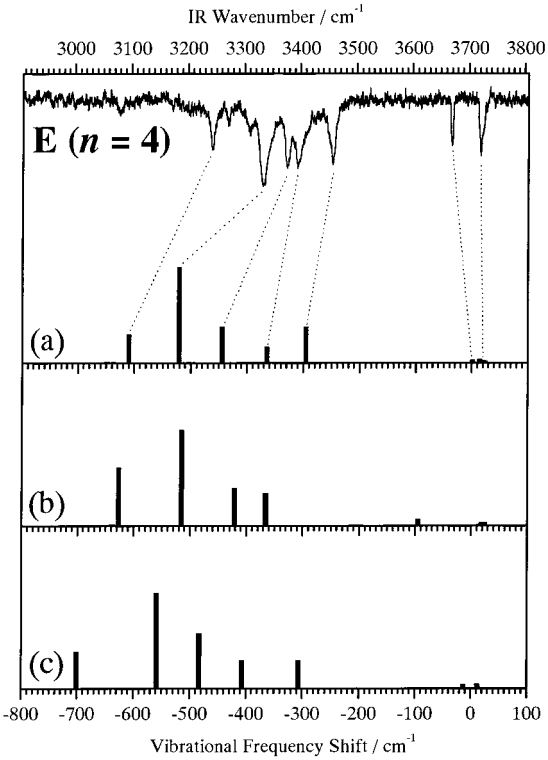

Figure 5. Comparison of the experimental and calculated N−H/O−H vibrational bands for species E [AD−$(H_2O)_4$]. The top panel shows the observed FDIR spectrum, and calculated spectra for the three isomers of $n = 4$ obtained at the B3LYP/6-31G(d,p) level are indicated as stick diagrams: (a) the bridged-type (**I**), (b) the N−H bonded chain-type (**II**), and (c) the N−H bonded cyclic-type (**III**) (see Figure 6 of paper I). Other details are the same as in Figure 2.

for species D. Although the calculated spectrum of the bridged isomer **I** best reproduces the observed feature among the rest three conformers, possibilities for isomers **IV** (the C═O bonded cyclic type) or **V** (the N−H bonded cyclic type) as the observed species cannot be ruled out. On the other hand, the $^1(\pi,\pi^*)$ spectral shift analysis performed in paper I has revealed that the calculated red shifts of isomers **IV** and **V** are much smaller than the experimental value of species D, and only isomer **I** well reproduces the observed shift within 50 cm^{-1}. Thus, experimental and computational results for vibrational spectra and those for spectral shifts in electronic transitions are complementary and their combination is crucial to structural determination of larger-size clusters containing a bifunctional solute molecule.

It should be noted that quantitative correspondences between the calculated (for the conformer **I**) and observed frequency shifts of the lowest three hydride stretches are not too good: the calculated bands separate each other more widely compared with the observed spectrum. This should be because DFT calculations using the B3LYP functional tend to overestimate the frequency shifts of H-bonded stretching vibrations.[4] It has been already shown that such overestimation can be improved by including higher order electron correlation effects.[4] In addition, the shift for the lower frequency band (3688 cm^{-1}) among the two in the free O−H region could not be reproduced well by calculation (see Figure 4). The present calculation level, i.e., B3LYP/6-31G(d,p), could not yield a sufficient flexibility to the water bridge, and one of the O−H bonds of water #2 is not allowed to interact with the π cloud of AD. Nevertheless, judging from the spectral features of the 3688 cm^{-1} band, e.g., small frequency shift of −19 cm^{-1}, modest intensity, and narrow breadth, this band is considered to be the stretch of the O−H bond of water #2, which is weakly interacting with the π aromatic ring of AD. To reproduce these observed features by calculations, inclusion of more diffuse functions in basis sets would be necessary.

The conclusive assignments of the O−H and N−H stretching vibrations in the $n = 3$ cluster (species D) are listed in Table 1. The four H-bonded stretch modes (3385, 3435, 3481, and 3509 cm^{-1}) in the observed spectrum are assigned to the concerted motions involving several H-bonded O−Hs of water(s) and/or the H-bonded N−H of AD, which form the bridge between the C═O and N−H sites. These "bridge" vibrations are discussed in some detail in the next section. Among the two highest frequency bands (3688 and 3724 cm^{-1}), the latter band with doubled intensity is assigned to an overlap of two independent free O−H stretches of water #1 and #3, and the other is assigned as the π-bonded O−H stretch of water #2 as mentioned above.

(4) AD−$(H_2O)_4$. Figure 5a−c shows the calculated IR spectra of AD−$(H_2O)_4$ **I**−**III**, respectively, in comparison with the FDIR spectrum of species E. The calculated O−H and N−H stretching vibrations of the bridged-type isomer **I** and the N−H bonded cyclic-type isomer **III** are similar, even though their molecular structures are quite different from each other. These two clusters exhibit five intense H-bonded bands with shifts ranging from −710 to −290 cm^{-1}, and one π-bonded and three free O−H bands with shifts between −20 and +30 cm^{-1}. On the other hand, the calculated IR spectrum of the N−H bonded chain-type isomer **II** shows four intense H-bonded bands between −630 and −360 cm^{-1} in shifts, one π-bonded O−H

stretch at −95 cm^{-1} shift, and four free O−H stretches around +20 cm^{-1} shift. In the observed FDIR spectrum of species E, *five* intense bands are identified in the red-shifted region (3200−3480 cm^{-1}), excluding the assignment to AD−$(H_2O)_4$ **II**. This is consistent with the fact that isomer **II** is the least stable among the three as shown in paper I. Both of the calculated spectra for the isomers **I** and **III** indicate reasonably good match-up with the observed spectrum, although the red shifts in the H-bonded stretches are systematically overestimated at this level of theory, as mentioned before. Again, this onerous problem has been resolved by collaboration with the spectral-shift analysis described in paper I. The calculated spectral red shifts in the (π,π^*) electronic excitation of isomer **I** and **III** (−1764 and −498 cm^{-1}, respectively) are much different, and the former well reproduces the experimental value of −1589 cm^{-1}. Hence, we can safely conclude the geometrical structure of species E to be the bridged form (**I**). This is consistent with the energy ordering of two isomers **I** and **III**, i.e., isomer **I** is more stable than isomer **III** (see Table 2 in paper I). As will be thoroughly described in paper III, excited-state dynamics in species E is also consistent with the structural assignment to the bridged form. Its fluorescence lifetime from the $^1(\pi,\pi^*)$ origin is 3 orders of magnitude longer than that of bare AD. This is because cluster formation suppresses the rapid nonradiative decay in the AD chromophore, and the H-bonding to the carbonyl group of AD is essential to effect the nonradiative processes. Such an H-bonding interaction exists in the bridged form (**I**) but not in the N−H bonded cyclic form (**III**).

Band assignments of the observed FDIR spectra are listed in Table 1. The five intense bands in the H-bonded O−H stretching region are also assigned to the concerted motions of H-bonded O−H and/or the H-bonded N−H as in the case of $n = 3$. The sharp 3670 cm^{-1} band is assigned to the π-H-bonded O−H stretch of water #3, and the highest frequency band is assigned to an overlap of three free O−H stretches of water #1, #2, and #4.

(5) AD−$(H_2O)_5$. Figure 6 shows the comparison of the observed FDIR spectrum of species F with the calculated ones for AD−$(H_2O)_5$ **I**−**III**. As all of the three conformers contain six strong H-bonds, i.e., σ-type or C═O bonded π-type, their calculated IR spectra all exhibit six intense bands with shifts reneging from −900 to −290 cm^{-1}. The number matches with that for the H-bonded stretches observed in 3200−3500 cm^{-1}, if the clump at ≈3350 cm^{-1} is considered as three bands. The minor difference in the calculated spectra is the number of π-H bonds bound to the AD aromatic rings: two for the isomers **I** and **III** while one for **II**. Though the global feature of the observed spectrum is reasonably resembled by any of the calculated spectra, quantitative correspondence is rather dubious due to the limited accuracy in calculations applied in the present study.

To make a definitive structural assignment of species F, the following arguments are to be presented. First, the experimental large red shift (1649 cm^{-1}) in the $^1(\pi,\pi^*)$ electronic transition is not reproduced by the N−H bonded cyclic isomer **III** at all, but the bridged isomers **I** and **II** reproduce very well, as have been discussed in paper I. Second, the fluorescence lifetime of species F is also 3 orders of magnitude longer than that of bare AD. This indicates the existence of H-bonding interaction involving the carbonyl group of AD, which is against the possibility of the "N−H bonded cyclic" form **III**. Third, bridged isomer **I** is the most stable conformer among the three, and the energy margin between **I** and **II** is larger than 1 kcal/mol at the present calculation level (see Table 2 of paper I). Fourth, the

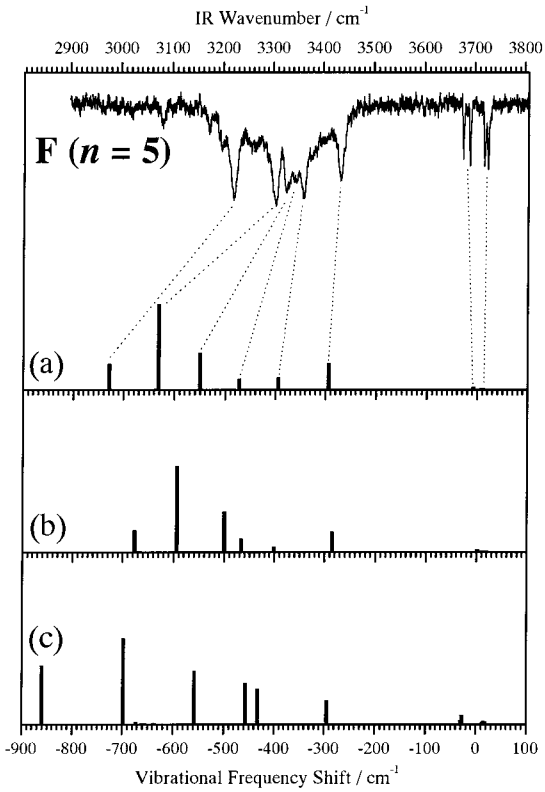

Figure 6. Comparison of the experimental and calculated N−H/O−H vibrational bands for species F [AD−$(H_2O)_5$]. The top panel shows the observed FDIR spectrum, and calculated spectra for the three isomers of $n = 5$ obtained at the B3LYP/6-31G(d,p) level are indicated as stick diagrams: (a) the bridged-type (**I**), (b) the bridged-type (**II**), and (c) the N−H bonded cyclic-type (**III**) (see Figure 7 of paper I). Other details are the same as in Figure 2.

two bands at 3678 and 3691 cm^{-1} in the observed FDIR spectrum show relatively large red shifts as free O−H stretches and are probably assigned to the π-H bonds to the AD aromatic rings. This structural feature well agrees with AD−$(H_2O)_5$ **I** or **III** but not with **II**. Therefore, we conclude that the AD−$(H_2O)_5$ cluster identified in the present study, i.e., species F, should be assigned to the bridged form **I**, as in the case of AD−$(H_2O)_4$. Corresponding band assignments of the observed FDIR spectra are listed in Table 2. Vibrational motions corresponding to the six H-bonded bands are identified as "bridge" vibrations.

(6) AD−$(H_2O)_n$ ($n \geq 6$). As discussed in the preceding section, the O−H stretching transitions due to DD water molecule(s) have been observed in the FDIR spectra of the larger clusters (H, J, L, M, and N). Here we briefly perform the structural characterizations of species H ($n = 6$) and other higher clusters. The geometrical structures of the hydrated AD clusters with $n = 3-5$ (species D−F) have been assigned to the bridged-type conformation, in which the $^1(\pi,\pi^*)$ transitions of the AD chromophore show extremely large spectral red shifts. These results give a valuable hint on the H-bonding topologies of the larger hydrated AD clusters. Because their $^1(\pi,\pi^*)$ transitions are further red-shifted relative to species D−F, we can securely speculate that their geometrical structures should be also of *bridged* type as the smaller size clusters (species D−F, $n = 3-5$).

In the observed FDIR spectrum of species H, two characteristic bands are observed at 3500 and 3564 cm^{-1}. The transition frequencies of these bands well correspond to the symmetric and antisymmetric vibrations of a double-donor (DD) water molecule (DDν_1 and DDν_3), which have been typically

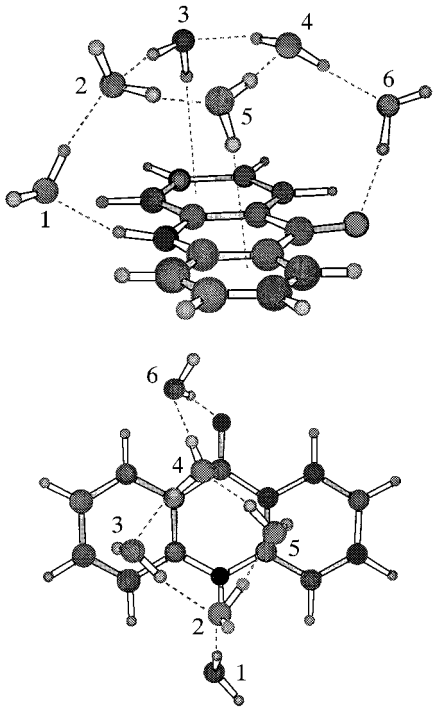

Figure 7. Probable geometry for species H [AD−$(H_2O)_6$] calculated as a stable isomeric form at the B3LYP/6-31G(d,p) level. Possible H-bonds are marked with broken lines, and numbering of each water molecule is given.

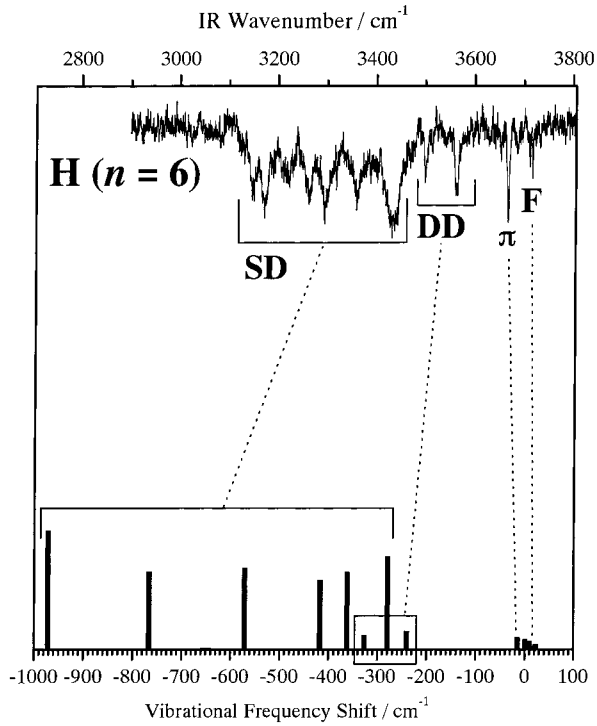

Figure 8. Comparison of the experimental and calculated N−H/O−H vibrational bands for species H [AD−$(H_2O)_6$]. The top panel shows the observed FDIR spectrum, and the calculated spectrum for the bridged form obtained at the B3LYP/6-31G(d,p) level (see Figure 7) is indicated as a stick diagram. Dotted lines connect the corresponding groups of vibrational fundamentals with the same type, i.e., single-donor (SD), double-donor (DD), π-bonded (π), and free (F) hydride-stretching modes.

observed in 3450−3650 cm^{-1} with modest intensity.[3,5,14] Furthermore, the band at 3668 cm^{-1} should be assigned to π-bonded O−H stretch(es). Therefore, one DD H_2O and at least one π-bonded O−H bond should exist in the H-bonding network in species H. In addition, only two weak bands are identified in the free O−H region of the FDIR spectrum, suggesting that only a few free O−H bonds exist in this species. Figure 7 shows one stable bridged-type structure of AD−$(H_2O)_6$ obtained at the B3LYP/6-31G(d,p) optimization. In this structure, four water molecules (#2−#5) make a cyclic unit, in which water #4 acts as a DD and waters #3 and #5 are π-H bonded to the AD aromatic rings. The cyclic water tetramer is propped by the other two water molecules (#1 and #6), which are bound to the N−H and C═O sites of AD, respectively. Only three free O−H bonds (#1, #2, and #6) exist in this structure. These features of the bridged conformer of $n = 6$ are in good agreement with the H-bonding topology of species H estimated from its IR spectrum as described above. The calculated vibrational spectrum for this conformer at the B3LYP/6-31G(d,p) level is shown in Figure 8 along with the observed FDIR spectrum of species H. Quantitative correspondence between them is far from satisfying: frequency shifts of single-donor (SD) O−H and DD O−H stretches are largely overestimated. Detail assignments of each bands are difficult to carry out at the present level of calculation, but qualitative correspondence between the observed and calculated spectra can be made for characteristic features of SD-, DD-, π-, and free O−H stretching modes, as shown with dotted lines in Figure 8. Therefore, we conclude that this bridged-type conformer is the most probable structure of species H.

Since mass assignments of the other larger clusters have not been conducted, we cannot perform their definitive structural assignments at present. However, we surmise that bridged-type structures with structural motif of the "cyclic bridge" for $n =$ 6 (species H) would be also favored in larger hydrated AD clusters ($n \geq 7$), since water clusters consisting of rings with four water molecules have been identified as especially stable by molecular orbital calculations.[25] For example, a cubic bridged-type structure, in which another water tetramer is bound to AD−$(H_2O)_6$, has been obtained as a stable conformer for $n = 10$ at the RHF/6-31G level. It is noted that eight water molecules in this conformer make a cube, which is essentially the same as the most-stable form identified in water octamer[26,27] or benzene-$(H_2O)_8$.[8]

5. Discussion

5.1. Evolution of H-Bonding Networks in the Hydrated Clusters of AD. In the present study, the stepwise evolution of hydration structure in fluorescent AD−$(H_2O)_n$ has been clarified by the combined use of experiments and calculations: in the early stage of hydration, i.e., $n = 1$ and 2, water units are bound to the C═O site, the C═O and N−H sites come to be bridged by a single water chain for the next solvation step in $n = 3-5$, and water bridges are extended into 2D/3D networks at higher aggregation level with $n \geq 6$. It is noted that only a single isomer has been identified for each cluster size with $n = 1-6$ via the fluorescence-excitation measurements, despite that the DFT calculations have identified several isomeric forms with similar binding energies for each cluster size. Of course, the size evolution in geometry of the observed species is mainly controlled by the relative stabilities for stable isomers. Here we discuss the geometrical crossovers in relation to the possibility for the coexistence of different isomeric forms.

The DFT calculations have shown that the N−H bonded hydrates of AD for $n = 1-3$ [AD−$(H_2O)_1$ **II**, AD−$(H_2O)_2$ **II**, and AD−$(H_2O)_3$ **III**] are more stable than the corresponding C═O bonded hydrates by ≈1−2 kcal/mol at the B3LYP/6-31G-(d,p) level with BSSE corrections. Thus these N−H bonded

forms should also exist with appreciable abundance in supersonic expansions, but have *not* been identified in the fluorescence-excitation (FE) spectrum. As will be discussed thoroughly in paper III, this experimental observation correlates to a remarkable dependence of intersystem crossing (ISC) rates of the AD chromophore on solute−solvent conformation: when water molecule(s) are *not* bound to the C═O site, rapid ISC processes are *not* suppressed so that the N−H bonded forms are virtually nonfluorescent as bare AD. This dynamical consequence is the origin of the absence of any N−H bonded hydrates in the *FE* spectrum. When we utilize a sensitive ion-detection method for molecules in triplet-states, i.e., delayed ionization,[28−31] (probably more than one) nonfluorescent hydrates, which did not appear in the FE spectrum, have been detected in the AD−$(H_2O)_1^+$ channel. This issue will be further discussed in detail in the following paper. The definitive structural assignments of these new species must await further experiments, e.g., ion-detected IR spectroscopy with the delayed ionization scheme, but we are convinced that these species are N−H bonded isomers of AD with n in the range of 1−3.

Because all of the C═O bonded forms are strongly fluorescent as exemplified for $n = 1$ and 2, the observed geometrical transition from the C═O bonded form to the bridged one between $n = 2$ and 3 indicates that the former should be much less abundant under the jet-cooled conditions for $n \geq 3$. This implies that the C═O bonded isomer becomes less stable than the bridged one for the larger clusters which is consistent with the results of the DFT/B3LYP/6-31G(d,p) calculations for $n = 3$, where binding energy of bridged isomer is >2 kcal/mol greater than that of C═O bonded chain isomer (19.8 and 17.7 kcal/mol with BSSE corrections for the isomers **I** and **II**, respectively; see Table 2 of paper I). However, enegetics alone, i.e., relative stabilities, cannot explain the absence of the C═O bonded isomers, because the less stable C═O bonded forms *do* coexist with the more stable N−H bonded forms for $n = 1$ and 2. Thus we also have to consider kinetic constraint for interconversion between different isomers: if the potential barrier separating them is high enough, the relaxation to the lower species cannot proceed effectively, keeping substantial population for the less stable form even under jet-cooled conditions. This is the case for the coexistence of the C═O and N−H bonded isomers with $n = 1$ and 2. The interconversion between them requires a movement of the whole water unit from one site to the other, which must be energetically very unfavorable. On the other hand, the absence of the C═O bonded AD−$(H_2O)_3$ **II** indicates the efficient relaxation of the species into the more stable bridged form **I** (and/or the N−H bonded form **III**), implying sufficient flexibility in the water unit in the isomer **II**. This may be reasonable since one end of the water unit is bound strongly to the C═O site but the other side interacts only weakly with the 2-hydrogen of AD.

Judging from the large spectral red shifts in the $^1(\pi,\pi^*)$ transition for $n \geq 6$, no isomeric forms other than bridged types exist for the larger hydrated clusters of AD under the supersonic expansion condition. This should be quite equitable as the bridged forms are the most stable, even for the smaller sizes ($n = 4$ and 5). The geometrical transition from the linear chain to the structured bridge at $n = 6$ can be rationalized by additional stability from a σ-H bond between waters as well as another π-H bond to the AD aromatic ring, while the linear chain with six water molecules is too long to bridge the C═O and N−H sites while keeping the contacts with π-electrons.

5.2. Hydration Structures at C═O and N−H Groups. On the basis of the present results, it is intriguing to assess the characteristics of water-solvation structures at the proton-accepting C═O and the proton-donating N−H groups. Several striking differences have been identified in geometrical structures of water moieties associated to the two H-bonding sites. In the C═O bonded chain-type structures, e.g., AD−$(H_2O)_2$ **I** and AD−$(H_2O)_3$ **II**, waters lie approximately in the AD molecular plane and surround the edge of the aromatic ring of AD. On the other hand, water chains bound to the N−H site are out of the AD molecular plane to bridge the N−H site and the π-clouds of AD [see AD−$(H_2O)_2$ **II** and AD−$(H_2O)_3$ **III**]. This contrast in solvation structure is related to so-called "cooperative effects".[32] Once a water molecule is bound to an H-accepting (or donating) site, its H-accepting (donating) ability becomes stronger due to the polarization in its O−H bond. Such an enhancement in H bonding is cooperative since the bond polarization is increased as more water molecules acting as a H-donor/acceptor are gathered, though the increase should become saturated for a certain aggregation level.[33] Therefore, a water chain whose one end is bound to a rather strong H-accepting site, e.g., C═O, tends to be an H acceptor at the other end. This is actually seen in the C═O bonded chain forms with $n = 2$ and 3, in which the oxygen atom of the terminal water is weakly interacted with the 1- or 2-hydrogen of the AD aromatic ring. Situation for a water chain bound to an H-donating site is completely reversed: the chain is predominately terminated as an H donor, such as those in the N−H bonded-chain form with $n = 2-5$, which make H bonds to the π-cloud of AD. These structural motifs should be universal for other hydrated clusters containing an aromatic molecule with polar functional group(s), and have actually been identified in previous studies on clusters of benzonitrile (with an H-accepting CN group),[23] acridine (with an azo-nitrogen as an acceptor),[18] and indole (with an H-donating N−H).[10,12] Furthermore, the H-bonding structures at the C═O and N−H groups thus identified can be a molecular-level basis for understanding of local hydration structures at the functional groups in various biological systems.

Similar to the chain-type clusters, a sharp contrast in structural motifs has also been identified in the C═O and N−H bonded cyclic-type clusters. In the C═O bonded cyclic-type AD−$(H_2O)_3$ **IV**, the molecular plane of the cyclic water trimer is nearly perpendicular to that of AD. On the other hand, in the N−H bonded cyclic-type AD−$(H_2O)_3$ **V**, the water trimer is substantially tilted toward the AD aromatic ring to form a π-H bond. In this case, it is difficult to make a simple explanation for the difference, as the polarization of the O−H bonds should not be affected so much by the relative orientation of the cyclic waters against the AD molecule. We only note that the oxygen atoms of waters #1 and #3 in the isomer **IV** locate nearly at the same positions of those of water # 1 and #2 in the C═O bonded AD−$(H_2O)_2$ **I**, and the orientation of waters #1 and #2 in the isomer **V** resembles that of the water dimer (#1 and #2) in the N−H bonded AD−$(H_2O)_2$ **II**. This leads to a speculation that the interaction between the polar site and water #1 is the predominant factor to determine the conformation in cyclic-type clusters: in order to keep the maximum interaction, the O−H bond of the water should be directed strictly to the carbonyl lone-pair electrons in the C═O bonded form **I**, while the H-bonding between the water and the N−H site is more flexible and thus another water is allowed to make a π-H bond to gain additional stability.

5.3. Relative Stabilities for Different Conformations. In the present study, a number of conformations have been identified as minimum-energy structures for a given cluster size

by the DFT calculation. For the clusters with more than one water molecule, the above-mentioned cooperative effects play an important role to determine the relative stabilites among the conformers. The calculated binding energies of water and the C═O or N−H site in AD with BSSE and *no* ZPVE corrections (6.1 and 6.4 kcal/mol, respectively) are >2 kcal/mol greater than the water−water binding energy (3.7 kcal/mol). Nevertheless, the isomers for $n = 2$ with water units bound to the C═O and N−H sites (**I** and **II**) are calculated to be more stable than isomers **III** and **IV** in which the two sites are H bonded by waters independently (see Table 2 of paper I). The separately bonded forms also show a cooperative effect due to the polarization of the AD chromophore as mentioned in paper I, but the polarization in the water dimer has predominant effects to increase both the water−water and water−solute interactions.

If water units can connect between strongly H-accepting and H-donating sites, the cooperative effects are maximized to give a substantial stability to the system. This situation is partly fulfilled in the most stable N−H bonded forms for $n = 2$ (**II**) and $n = 3$ (**III**), despite the relatively low H-accepting ability in the π cloud which is bound by the other end of the water chain. Of course, the bridged conformation for $n = 3-5$ is best to be categorized in this case. The isomers for $n = 3$ of this type (**I**) are calculated as almost isoenergetic to the C═O bonded-type **II** at the present level of theory but should be more stable as mentioned in section 5.1. Calculations with sufficiently diffuse functions will provide the system with more flexibility, leading to the reduction of the strain in the water bridge which should now spoil the stability from the cooperative effect. Also for other hydrated aromatic clusters, various bridged structures have recently been studied[10,12,24,34−36] and such water bridges are realized as a common feature for clusters containing a solute molecule with multiple H-bonding sites.[34−36]

The present DFT calculations have predicted that the cyclic-type conformers for $n = 3-5$ are almost isoenergetic to or slightly unstable than the bridged forms. However, more extensive calculation should reveal that the latter is substantially more stable than the former due to the structural relaxation given by extended molecular orbitals. This estimation is in accord with the present experimental result that no conformers in which cyclic water units bound to the polar H-bonding sites have been observed. Similar observations have been experienced for the acridine$-(H_2O)_3$ (ref 18) and the benzonitrile$-(H_2O)_3$ clusters.[23] This is in contrast to hydrated clusters of aromatic hydrocarbons, in which cyclic conformation of water units has been considered as most stable. For example, benzene$-(H_2O)_3$ has been identified to possess the cyclic water trimer bound to the π cloud of the aromatic ring.[3,4] This may be because the polarization in the water units induced by the solute molecule (e,g., benzene) is insufficient to gain an additional stability at the π-H bond, which originates the structural change of the water units from that of the free water trimer[37] to a linear chain.

5.4. Bridged Structures and Their Vibrations. Since H-bonded bridges between the H-accepting and H-donating sites might play a particularly important role in excited-state proton transfer (ESPT) reactions, they have become a subject for extensive experimental and theoretical studies.[35,36,38,39] One of the most representative examples is a recent study by Leutwyler and co-workers on the 7-hydroxyquinoline$-(H_2O)_n$ clusters, in which water chains composed of up to four water molecules bridge the O−H group and the N atom of the solute.[35] They investigated the intermolecular vibrations of 7-hydroxyquinoline-$(H_2O)_2$ in both the S_0 and S_1 states in order to explore the correlation between H-bonded water bridges and ESPT reactivity.[36] In the present work, the FDIR and DFT results have led to confirm the bridged structures for the hydrated AD clusters with $n = 3-5$, in which water chains composed of three to five water molecules bridge between the C═O and the N−H groups. Although we have not examined whether the ESPT occur or not in these hydrated AD clusters, it is important to survey some characteristic features in the bridged-type structures.

The $^1(\pi,\pi^*)$ origins of the bridged AD$-(H_2O)_n$ with $n = 3$, 4, and 5 show very large red shifts relative to bare AD (1364, 1589, and 1649 cm^{-1}, respectively), which have been already rationalized by the HOMO−LUMO energetics in paper I. These large red shifts correspond to 3.9−4.7 kcal/mol increase in H-bond dissociation energy upon electronic excitation. Comparably large shifts have been observed for the bridged hydrates of 7-hydroxyquinoline with $n = 2-4$.[35,36] The drastic increase of the H-bonding interaction by electronic excitation often induces structural change in the water chain along the bridge coordinates, which results in the enhancement of Franck−Condon activities for intermolecular vibrations along the coordinates.[12,35] The UV−UV HB measurements of AD$-(H_2O)_n$ ($n \geq 3$) have shown that the low-frequency progressions (20−30 cm^{-1}) involving one or more intermolecular vibrations begin to appear at this aggregation level. Therefore, these progressions might be due to the water chain (intermolecular) vibrations just mentioned.

The DFT calculations performed in the present study have revealed that H-bonded vibrational modes of the bridged-type structures are described as concerted motions of several H-bonded bonds along the water bridge; such vibrational modes have recently been termed as "bridge vibrations".[12,35,36] One notable feature in the bridge vibrations of $n = 3-5$ is that the bond showing the largest vibrational amplitude is moved from the N−H bond to the C═O bonded O−H bond along the bridge, as the vibrational frequency of the mode becomes larger. For example, the lowest bridge vibration (3385 cm^{-1}) of $n = 3$ is assigned as a concerted motion of the N−H bond of AD and the O−H bond of water #1: the relative magnitudes of the vibrational displacements are approximately 75:25 for the two bonds. The other three bridge vibrations (3435, 3481, and 3509 cm^{-1}) are also the concerted motions of several bonds, and the relative displacements in these modes are: N−H → O/O−H(#1) → O/O−H(#2) → O (20%/60%/20%), O−H(#1) → O/O−H(#2) ← O/O−H(#3) ← O (25%/64%/11%), and O−H(#2) → O/O−H(#3) ← O stretch (16%/84%), respectively, where → and ← denote the relative phase of the bond stretching motions. Similar trends are also identified in the bridge vibrations of the bridged-type conformers of $n = 4$ and 5 as listed in Table 2.

In general, red shift and increase in intensity for hydride stretches induced by H-bond formation well correlate with H-bond strength.[18,23] Particularly, in the case of the hydrated clusters of chain-type structures, the most red-shifted transitions for the hydride stretches have been identified as the most intense ones.[18,23] The present FDIR spectrum of $n = 2$ (species C) serves as another example. In contrast to this, the *second* lowest bands (3435, 3335, and 3306 cm^{-1}) are the most intense in the FDIR spectra of $n = 3-5$ (species D−F). However, by careful consideration, it is realized that the above-mentioned tendency also holds for the FDIR spectra of $n = 3-5$ as follows. The lowest bands (3385, 3243 and 3222 cm^{-1}) are mostly contributed by the N−H stretch of AD and the shifts of these bands relative to free N−H stretch are −93, −235, and −256 cm^{-1}, respectively. On the other hand, the most intense bands (second red-shifted bands) of $n = 3$, 4, and 5 are practically due to the

O−H stretches of waters and their frequency shifts relative to ν_1 (3657 cm^{-1}) of free water[22] are −222, −322, and −351 cm^{-1}, respectively. Therefore, it is recognized that the most intense H-bonded O−H bands are actually more red-shifted than the lowest bands (the H-bonded N−H bands).

6. Conclusions

In the present paper II, FDIR spectroscopy of AD and 10 of its hydrated clusters, AD−$(H_2O)_n$ (n = 1−5 and more) have been described. The observed spectra have shown characteristic features, which are changed in accord with the hydration aggregation level of the clusters as follows. In the n = 1 and 2 clusters, the N−H stretching mode has been located at the same position as the bare AD, and all of the O−H stretching bands of the solvent(s) have been assigned to those of water molecules acting as single proton donors. As the next solvation step, no free N−H stretch is observed and single-donor H-bonded O−H stretches are further developed in the red-shifted region for the n = 3−5 clusters. For $n \geq 6$, O−H stretching bands due to double-donor (DD) water(s) appear, and clusters probably with $n > 6$ show more than one pair of DD O−H bands. These experimental observations provide concrete support, and more detailed information about the stepwise evolution of hydration structure in AD−$(H_2O)_n$, which has been predicted by the (π,π^*) spectral-shift analysis and DFT calculations presented in paper I. Particularly, the FDIR spectra have definitively assigned the observed fluorescent n = 1 and 2 clusters as the C═O bonded form among the two possible stable conformations, which cannot be differentiated only by the spectral-shift analysis. It is also confirmed that a single water chain bridges the C═O and N−H sites above the AD aromatic rings in the observed clusters with n = 3−5. Vibrational characters of H-bonded hydride stretching modes along the bridge are considered by comparing the experimental spectra and DFT calculations. For $n \geq 6$, water bridges become apparently branched and probably form 3D cages at higher aggregation level. These H-bonding topologies for hydrated clusters, especially with bifunctional solute molecules, are discussed in relation with their stabilities.

Acknowledgment. The present work has been supported by the Joint Studies Program (1998−1999) of the Institute for Molecular Science and Grants-in-Aid (Nos. 08454177, and 10440172) from the Ministry of Education, Science, Culture, and Sports of Japan. Y.O. thanks the Mitsubishi Chemical Foundation and the Japan Securities Scholarship Foundation for financial support.

References and Notes

(1) Zwier, T. S. *Annu. Rev. Phys. Chem.* **1996**, *47*, 205.
(2) Tanabe, S.; Ebata, T.; Fujii, M.; Mikami, N. *Chem. Phys. Lett.* **1993**, *215*, 347.
(3) Pribble, R. N.; Zwier, T. S. *Science* **1994**, *265*, 75.
(4) Ferdericks, S. Y.; Jordan, K. D.; Zweir, T. S. *J. Phys. Chem.* **1996**, *100*, 7810.
(5) Watanabe, T.; Ebata, T.; Tanabe, S.; Mikami, N. *J. Chem. Phys.* **1996**, *105*, 408.
(6) Mitsuzuka, A.; Fujii, A.; Ebata, T.; Mikami, N. *J. Chem. Phys.* **1996**, *105*, 2618.
(7) Pribble, R. N.; Hagemeister, F. C.; Zweir, T. S. *J. Chem. Phys.* **1997**, *106*, 2145.
(8) (a) Gruenloh, C. J.; Carney, J. R.; Arrington, C. A.; Zweir, T. S.; Fredericks, S. Y.; Jordan, K. D. *Science* **1997**, *276*, 1678. (b) Gruenloh, C. J.; Carney, J. R.; Hagemeister, F. C.; Arrington, C. A.; Zweir, T. S.; Fredericks, S. Y.; Wood, J. T., III; Jordan, K. D. *J. Chem. Phys.* **1998**, *109*, 6601.
(9) Yoshino, R.; Hashimoto, K.; Omi, T.; Ishiuchi, S.; Fujii, M. *J. Phys. Chem. A* **1998**, *102*, 6227.
(10) Carney, J. R.; Hagemeister, F. C.; Zwier, T. S. *J. Chem. Phys.* **1998**, *108*, 3379.
(11) Barth, H.-D.; Buchhold, K.; Djafari, S.; Reimann, B.; Lommatzsch, U.; Brutschy, B. *Chem. Phys.* **1998**, *239*, 49.
(12) Carney, J. R.; Zwier, T. S. *J. Chem. Phys.* **1999**, *103*, 9943.
(13) Matsuda, Y.; Ebata, T.; Mikami, N. *J. Chem. Phys.* **1999**, *110*, 8397.
(14) Mitsuzuka, A.; Fujii, A.; Ebata, T.; Mikami, N. *J. Phys. Chem.* **1998**, *102*, 9779.
(15) Janzen, C.; Spangenberg, W.; Roth, W.; Kleinermanns, K. *J. Chem. Phys.* **1999**, *110*, 9898.
(16) Mons, M.; Robertson, E. G.; Snoek, L. C.; Simons, J. P. *Chem. Phys. Lett.* **1999**, *310*, 423.
(17) Graham, R. J.; Kroemer, R. T.; Mons, M.; Robertson, E. G.; Snoek, L. C.; Simons, J. P. *J. Phys. Chem. A* **1999**, *103*, 9706.
(18) Mitsui, M.; Ohshima, Y.; Ishiuchi, S.; Sakai, M.; Fujii, M. *Chem. Phys. Lett.* **2000**, *317*, 211.
(19) Omi, T.; Shitomi, H.; Sekiya, K.; Takazawa, M.; Fujii, M. *Chem. Phys. Lett.* **1996**, *252*, 287.
(20) Okuzawa, Y.; Fujii, M.; Ito, M. *Chem. Phys. Lett.* **1990**, *171*, 341.
(21) Frisch, M. J.; Trucks, G. W.; Schlegel, H. B.; Scuseria, G. E.; Robb, M. A.; Cheeseman, J. R.; Zakrzewski, V. G.; Montgomery, J. A.; Stratmann, R. E., Jr.; Burant, J. C.; Dapprich, S.; Millam, J. M.; Daniels, A. D.; Kudin, K. N.; Strain, M. C.; Farkas, O.; Tomasi, J.; Barone, V.; Cossi, M.; Cammi, R.; Mennucci, B.; Pomelli, C.; Adamo, C.; Clifford, S.; Ochterski, J.; Petersson, G. A.; Ayala, P. Y.; Cui, Q.; Morokuma, K.; Malick, D. K.; Rabuck, A. D.; Raghavachari, K.; Foresman, J. B.; Cioslowski, J.; Ortiz, J. V.; Stefanov, B. B.; Liu, G.; Liashenko, A. Piskorz, P.; Komaromi, I.; Gomperts, R.; Martin, R. L.; Fox, D. J.; Keith, T.; Al-Laham, M. A.; Peng, C. Y.; Nanayakkara, A.; Gonzalez, C.; Challacombe, M.; Gill, P. M. W.; Johnson, B.; Chen, W.; Wong, M. W.; Andres, J. L.; Gonzalez, C.; Head-Gordon, M.; Replogle, E. S.; Pople, J. A. Gaussian 98, Gaussian, Inc.: Pittsburgh, PA, 1998.
(22) Fraud, J. M.; Camy-Peret, C.; Maillard, J. P. *Mol. Phys.* **1976**, *32*, 449.
(23) Ishikawa, S.; Ebata, T.; Mikami, N. *J. Chem. Phys.* **1999**, *110*, 9504.
(24) Guchhait, N.; Ebata, T.; Mikami, N. *J. Chem. Phys.* **1999**, *111*, 8438.
(25) Lee, C.; Chen, H.; Fizgerald, G. *J. Chem. Phys.* **1995**, *102*, 1266.
(26) Buck, U.; Ettischer, I.; Melzer, M.; Buch, V.; Sadlej, J. *Phys. Rev. Lett.* **1998**, *80*, 2578.
(27) Sadlej, J.; Buch, V.; Kazimirski, J. K.; Buck, U. *J. Phys. Chem. A* **1999**, *103*, 4933.
(28) Duncan, M. A.; Dietz, T. G.; Liverman, M. G.; Smalley, R. E. *J. Phys. Chem.* **1981**, *85*, 7.
(29) Hiraya, A.; Achiba, Y.; Kimura, K. *J. Chem. Phys.* **1984**, *81*, 3345.
(30) Meijer, G.; Vries, M. S.; Hunziker, H. E.; Wendt, H. R. *J. Phys. Chem.* **1990**, *94*, 4394.
(31) Lipert, R. J.; Colson, S. D. *J. Phys. Chem.* **1990**, *94*, 2358.
(32) For example, Guo, H.; Karplus, M. *J. Phys. Chem.* **1992**, *96*, 7273. Guo, H.; Karplus, M. *J. Phys. Chem.* **1994**, *98*, 7104.
(33) Gregory, J. K.; Clary, D. C.; Liu, K.; Brown, M. G.; Saykally, R. J. *Science* **1997**, *275*, 814.
(34) Dickinson, J. A.; Hockridge, M. R.; Robertson, E. G.; Simons, J. P. *J. Phys. Chem. A* **1999**, *103*, 6938.
(35) Bach, A.; Leutwyler, S. *Chem. Phys. Lett.* **1999**, *299*, 381.
(36) Bach, A.; Coussan, S.; Leutwyler, S. *J. Chem. Phys.* **2000**, *299*, 381.
(37) Pugliano, N.; Saykally, R. J. *Science* **1992**, *257*, 1937.
(38) Bach, A.; Leutwyler, S. *J. Chem. Phys.* **2000**, *112*, 560.
(39) For example, Kohtani, S.; Tagami, A.; Nakagaki, R. *Chem. Phys. Lett.* **2000**, *316*, 88.